IOPscience iopscience.iop.org

Home Search Collections Journals About Contact us My IOPscience

Growth and Electronic Structure Studies of Metal Intercalated Transition Metal Dichalcogenides M_xNbSe_2 (M: Fe and Cu)

This content has been downloaded from IOPscience. Please scroll down to see the full text.

2013 Jpn. J. Appl. Phys. 52 10MC15

(http://iopscience.iop.org/1347-4065/52/10S/10MC15)

View the table of contents for this issue, or go to the journal homepage for more

Download details:

IP Address: 129.120.87.225
This content was downloaded on 07/02/2017 at 17:13

Please note that terms and conditions apply.

You may also be interested in:

Synthesis of Nitrogen-Doped Graphene by Plasma-Enhanced Chemical Vapor Deposition
Tomo-o Terasawa and Koichiro Saiki

Ion Acceleration by the Coulomb Explosion of Graphene
Chen Ming, Zheng-Zhe Lin, Yin Wang et al.

Magnetoelectronic and Optical Properties of Monolayer and AB-Stacked Bilayer Graphenes
Yen-Hung Ho, Yu-Huang Chiu, Jei Wang et al.

Systematic Investigation of the Intrinsic Channel Properties and Contact Resistance of Monolayer and Multilayer Graphene Field-Effect Transistor
Kosuke Nagashio, Tomonori Nishimura, Koji Kita et al.

Structure of Silicene Grown on Ag(111)
Chun-Liang Lin, Ryuichi Arafune, Kazuaki Kawahara et al.

Reduction of a Single Layer Graphene Oxide Film on Pt(111)
Seiji Obata, Hiroshige Tanaka and Koichiro Saiki

Interface Properties of Ag and Au/Graphene Heterostructures Studied by Micro-Raman Spectroscopy
Shiro Entani, Seiji Sakai, Yoshihiro Matsumoto et al.

Transmission Electron Microscopy and Raman-Scattering Spectroscopy Observation on the Interface Structure of Graphene Formed on Si Substrates with Various Orientations
Hiroyuki Handa, Ryota Takahashi, Shunsuke Abe et al.

Observation of Band Gap in Epitaxial Bilayer Graphene Field Effect Transistors
Shinichi Tanabe, Yoshiaki Sekine, Hiroyuki Kageshima et al.

Japanese Journal of Applied Physics **52** (2013) 10MC15 **REGULAR PAPER**
http://dx.doi.org/10.7567/JJAP.52.10MC15

Growth and Electronic Structure Studies of Metal Intercalated Transition Metal Dichalcogenides M_xNbSe_2 (M: Fe and Cu)

Yoonyoung Koh[1], Soohyun Cho[1], Joon Lee[2], Le-Xian Yang[3], Yan Zhang[3], Cheng He[3], Fei Chen[3], Dong-Lai Feng[3], Masashi Arita[4], Kenya Shimada[4], Hirofumi Namatame[4], Masaki Taniguchi[4], and Changyoung Kim[1]*

[1] *Department of Physics, Yonsei University, Seoul 120-749, Korea*
[2] *Sangmoon High School, Seoul 137-849, Korea*
[3] *Department of Physics, Surface Physics Laboratory (National Key Laboratory) and Advanced Materials Laboratory, Fudan University, Shanghai 200433, P. R. China*
[4] *Hiroshima Synchrotron Radiation Center, Hiroshima University, Higashihiroshima, Hiroshima 739-004, Japan*
E-mail: changyoung@yonsei.ac.kr

Received December 7, 2012; accepted February 26, 2013; published online October 21, 2013

There has been renewed interest in transition metal dichalcogenides (TMDs) as electronic materials. The modification of the electronic structures of TMDs by means of metal intercalation would be of interest in that respect. With this motivation, we have synthesized and performed angle-resolved photoemission studies on Fe- and Cu-intercalated TMD Fe_xNbSe_2 and Cu_xNbSe_2 with various x values. Fe_xNbSe_2 ($x = 0, 0.25$) and Cu_xNbSe_2 ($x = 0, 0.06$) were grown by the iodine vapor transport method. Intercalation and doping were confirmed by changes in c-axis lattice constant and electronic structure, respectively. A significant amount of electron doping from Fe and Cu was observed, as indicated in the ARPES data measured as the rigid downshift of bands. In addition, band folding was observed in Fe_xNbSe_2, for which the unit cell is doubled owing to the Fe order. However, the extra band folding expected from the antiferromagnetic order of Fe was not observed.
© 2013 The Japan Society of Applied Physics

1. Introduction

Graphene has many favorable properties as an electronic material, such as high mechanical strength and excellent thermal conductivity.[1–8] It has been demonstrated that single-layer graphene can be used to fabricate a field-effect transistor (FET).[9] On the other hand, the weakness of graphene as an electronic material is that it does not have a band gap. For this reason, there have been steady efforts to create a band gap using an external electric field in double-layer graphene[10–13] or by growing graphene on hexagonal boron nitride (h-BN).[14,15]

Other than graphene, attention has been paid to layered materials with layers weakly coupled by van der Waals force.[16] A few layers of those materials, obtained by an exfoliation method, can be used in the fabrication of devices. In that respect, a notable family of materials comprises transition metal dichalcogenides (TMDs) with strong intra-layer coupling but weak interlayer coupling. One advantage of using TMDs is that there are various selections unlike graphene. Recent reports on the successful fabrication of a FET using single- and double-layer MoS_2 brought even further attention to the possibility of using TMDs as electronic materials.[17]

The modification of physical properties of TMDs by inserting foreign atoms or molecules between weakly bonded layers would be of natural interest. The intercalation of metals atoms to modify electronic structures is of particular interest, because through it, we can control the doping process. $NbSe_2$, one of the best-known TMDs [see Fig. 1(a) for the crystal structure], is well known for its charge density wave (CDW) state below $T_{CDW} = 33.5$ K as well as its superconducting transition below $T_c = 7.2$ K.[18] The intercalation of metal atoms, such as V, Cr, Mn, Co, and Ni, was indeed found to modify physical properties, such as the CDW and superconducting states.[16,19–24] On the other hand, studies on the electronic structure change upon intercalation by means of direct methods, such as ARPES, are relatively rare.

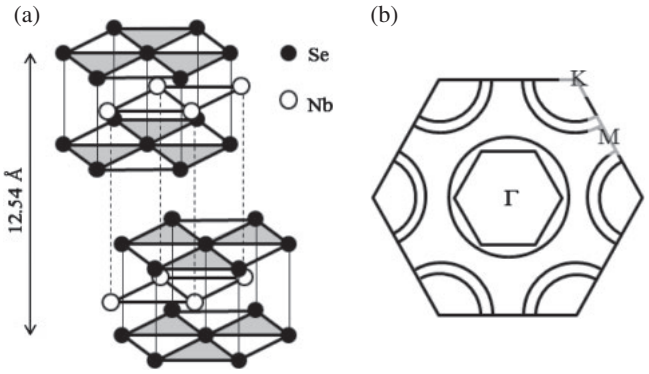

Fig. 1. (a) Crystal structure of $NbSe_2$. (b) Hexagonal BZ and schematic of FS topology. Special k-space points are also noted.

Motivated by this issue, we have synthesized Fe- and Cu-intercalated $NbSe_2$, Fe_xNbSe_2 ($x = 0, 0.25$), and Cu_xNbSe_2 ($x = 0, 0.06$). We find that both Fe and Cu donate electrons and downshift the original $NbSe_2$ bands. However, we find that Fe and Cu are not fully ionized, especially for Fe. Intercalated Fe is known to form a $2a_0$ superlattice as well as an antiferromagnetic (AF) order.[25–27] Although we see folded bands due to the $2a_0 \times 2a_0$ structural order, there is a lack of electronic structure modification due to the AF order. The latter implies that the interaction of the electrons in $NbSe_2$ and the Fe magnetic moment is fairly weak.

2. Experimental Methods

2.1 Crystal growth

Single crystals of $NbSe_2$ were synthesized by a conventional iodine vapor transport method.[28] The crystals were grown from pre-reacted polycrystalline samples. For the preparation of the starting material $Cu_{0.06}NbSe_2$, Cu, Nb, and Se

 © 2013 The Japan Society of Applied Physics

powders corresponding to the stoichiometric ratio were introduced into cleaned quartz tubes and sealed at a pressure of 10^{-2} Torr or lower. For the $Fe_{0.25}NbSe_2$ polycrystalline starting material, Fe, Nb, and Se powders at a ratio of 0.4 : 1 : 2[29] were sealed in evacuated quartz tubes. The ampoules were slowly heated from 25 to 800 °C at 4 °C/h and then annealed for 3 days at 800 °C.

For the single crystal growth, a charge of 2.5 g was introduced into ampoules and I_2 as a transport agent was subsequently added to the pre-reacted powder at an amount of 10 g/cm^3. Ampoules were then placed in a horizontal three-zone tube furnace with the hot and cold temperatures kept at 750 and 650 °C, respectively, and maintained for 2 weeks. The single-crystalline phase of the grown crystals was confirmed from (00*l*) X-ray diffraction (XRD) peaks. Intercalant concentration was determined from the *c*-axis lattice constant (lattice constants of $NbSe_2$, $Cu_{0.06}NbSe_2$, and $Fe_{0.25}NbSe_2$ are 12.547,[30] 12.58, and 12.67 Å, respectively).

2.2 Photoemission measurements

For $NbSe_2$ and $Cu_{0.06}NbSe_2$, ARPES data were taken using 21.2 eV light with a laboratory system equipped with Scienta R4000 and Gamma-data discharge lamp at 10 and 40 K. For $Fe_{0.25}NbSe_2$, data were taken at beamline 9A of the Hiroshima Synchrotron Radiation Center with a photon energy of 24 eV at 10 K. Samples were cleaved in situ at a pressure lower than 5×10^{-11} Torr. The energy resolutions were about 5 and 15 meV for the laboratory and beamline systems, respectively.

3. Results and Discussion

3.1 Doping effects

ARPES data from $NbSe_2$, $Fe_{0.25}NbSe_2$, and $Cu_{0.06}NbSe_2$ are plotted in Fig. 2. The left panel of Fig. 2(a) shows the Fermi surface (FS) map of $NbSe_2$ constructed by integrating a 20 meV energy window at approximately the Fermi energy. The symmetry and topology of the FSs are consistent with those of the Brillouin zone (BZ) and schematic FSs shown in Fig. 1(b). The right panel of Fig. 2(a) shows an image plot of the ARPES data along the Γ–K cut. The bands are two electron-like bands and there are 4 Fermi level crossings that extend from Γ to K, consistent with the schematic FS. Note that the bottom of the outer band is at a 200 meV binding energy.

When Cu atoms are intercalated between the weakly bonded layers of $NbSe_2$, they donate electrons. Such a process makes Cu_xNbSe_2 an electron-doped system. With extra electrons, the Fermi level shifts upward in the band structure or the bands shift downward. Since the FS pockets of $NbSe_2$ are hole pockets, the FSs should shrink. Plotted in Fig. 2(b) are the FS and Γ–K cut data of $Cu_{0.06}NbSe_2$. Comparing the FSs of the two systems, we find that the FS of $Cu_{0.06}NbSe_2$ is smaller than that of $NbSe_2$ as expected. It is easier to see the doping effect from the Γ–K cut data in the right panel. Note that the band bottom is now at 220 meV. This confirms that Cu intercalation indeed electron-doped $NbSe_2$.

Figure 2(c) shows the FS and Γ–K cut data of $Fe_{0.25}NbSe_2$. Although the overall FS shape is retained, one can immediately see that there is more electron doping

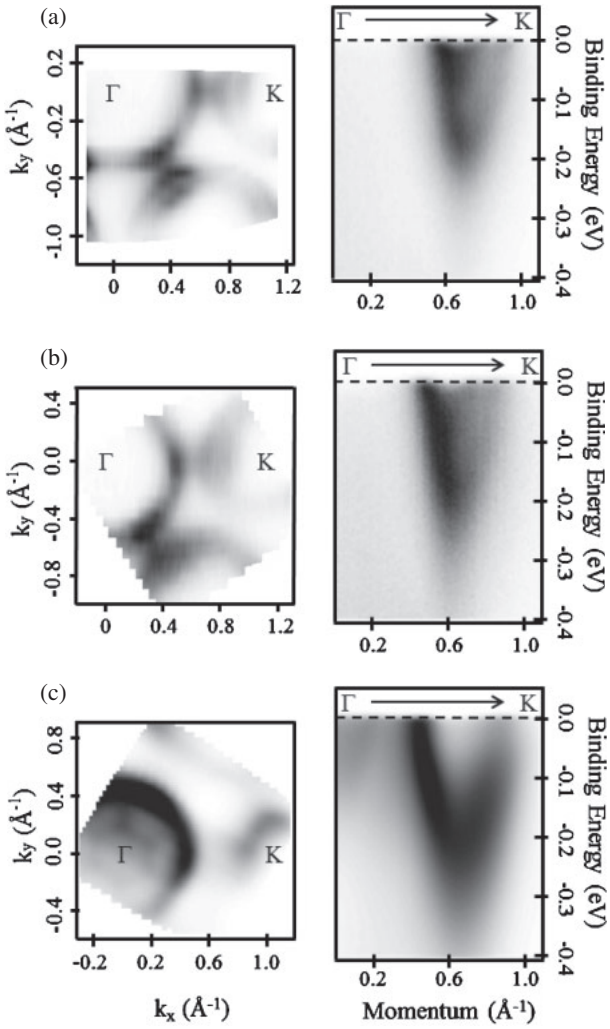

Fig. 2. ARPES spectra from (a) $NbSe_2$, (b) $Cu_{0.06}NbSe_2$, and (c) $Fe_{0.25}NbSe_2$. Left panels show FS maps in the first BZ constructed by integrating a 20 meV energy window at approximately the Fermi energy E_F, while right panels show ARPES data obtained along the Γ–K direction. For notations of Γ and K, refer to Fig. 1.

in this material. This is more evident in the Γ–K cut data for which the band bottom is now at 300 meV. The primary reason for the strong electron doping is simply the fact that there are more Fe atoms in $Fe_{0.25}NbSe_2$ than Cu atoms in $Cu_{0.06}NbSe_2$.

From the ARPES data in Fig. 2, we note two aspects of the data. We directly confirmed that electrons are indeed doped into $NbSe_2$ upon metal intercalation. From the estimated total FS area with respect to the entire BZ for $Cu_{0.06}NbSe_2$, the band filling is 0.58, which is larger than that for the pure system (0.51). In the case of $Fe_{0.25}NbSe_2$, the value is 0.73, which is much larger than that for the pure system. The values indicate that both Cu and Fe donate approximately one electron per atom and remain away from being fully ionized. This should be related to the fact that the metal hosting $NbSe_2$ is not as electronegative as typical anions, such as oxygen, and that we do not observe intercalant-derived bands. This is rather peculiar especially for $Fe_{0.25}NbSe_2$ considering the large amount of intercalated Fe and that Fe atoms are ordered. The overall effect of metal intercalation is a simple rigid shift of the $NbSe_2$ band structure.

© 2013 The Japan Society of Applied Physics

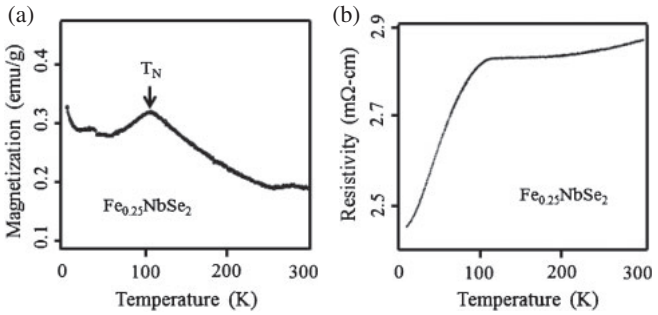

Fig. 3. Temperature-dependent (a) magnetization and (b) resistivity data from $Fe_{0.25}NbSe_2$. Magnetization was measured with the field direction perpendicular to the plane. The resistivity curve shows a sudden down turn at 106 K. A kink is observed at the same temperature for the magnetization curve.

3.2 Structure and AF ordering effects of Fe

Fe magnetic moments in $Fe_{0.25}NbSe_2$ order at a low temperature. Figure 3(a) shows a temperature-dependent magnetization curve of our crystals. The curve shows paramagnetic behavior above $T_N = 106$ K. Below T_N, the magnetization curve drops sharply, which is a typical behavior of an AF order. It also shows that magnetic moments lie in the plane as the magnetization was measured with the field perpendicular to the plane. The AF order is also reflected in the temperature-dependent resistivity data in Fig. 3(b). As temperature decreases, the resistivity suddenly drops below T_N. As the only difference observed above and below T_N is the magnetic order, such resistivity behavior implies that electrons in $Fe_{0.25}NbSe_2$ strongly interact with Fe magnetic moments. The contribution of fluctuating Fe magnetic moments to the resistivity above T_N decreases when Fe magnetic moments order below T_N.

Intercalated Fe atoms also order, as shown in Fig. 4. Shown in Fig. 4(a) are projections along the *c*-axis in a single $NbSe_2$ layer (left) as well as FSs (right). As Fe atoms are intercalated, they form an ordered phase, as shown in Fig. 4(b). As a result, the size of the unit cell quadruples, as indicated by the dotted tetragon. As the unit cell enlarges, the BZ shrinks. From a different view, one can say that bands should be folded. Considering the fact that the band structure should repeat itself when translated by reciprocal lattice vectors, one can construct the folded bands by translating original bands using reciprocal lattice vectors. So obtained FSs are drawn as dashed curves in the right panel of Fig. 4(b).

A rather complex resulting FS structure should be observed in the FS map. In fact, there is an indication of such folded bands in Fig. 2(c). In the FS map in Fig. 2(c), near the Γ point, there is a small weak hexagonal FS, which is formed by folded bands. However, such an FS is not observed in the $NbSe_2$ and $Cu_{0.06}NbSe_2$ data in Figs. 2(a) and 2(b), respectively. To investigate the folding effect in the electronic structure more closely, we plot ARPES data near the Γ point in Fig. 5. An electron-like band centered at the Γ point is evident. This band was originally near the M point of the BZ but was scattered in the Γ point region owing to the extra modulation induced by the ordered Fe atoms. The right panel of Fig. 5 shows selected momentum distribution curves of the data in the left panel. Two peaks

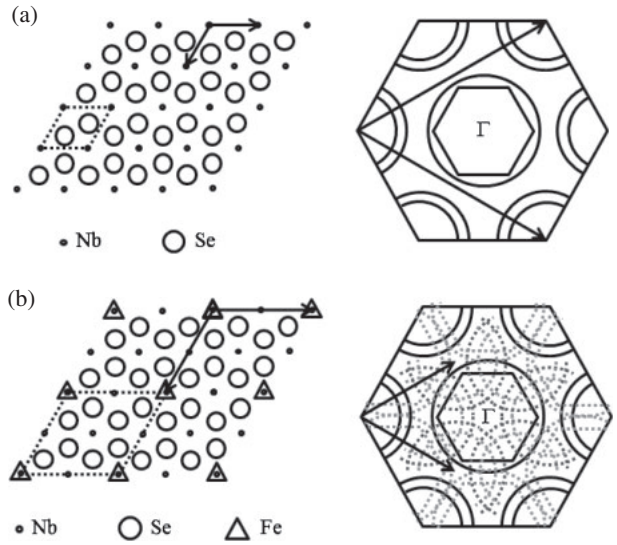

Fig. 4. Projection along *c*-axis of atomic arrangements in a single $NbSe_2$ layer (left), and FSs (right) of (a) $NbSe_2$ and (b) $Fe_{0.25}NbSe_2$. 2D unit cell and primitive translation vectors are denoted by dashed quadrangles and solid arrows, respectively, in the left panels, while reciprocal lattice vectors are denoted by solid arrows in the right panels. For the FSs of $Fe_{0.25}NbSe_2$, grey dashed lines indicate the folded FSs of the original ones.

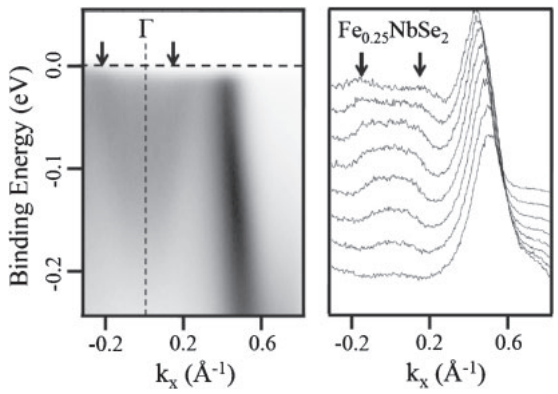

Fig. 5. $Fe_{0.25}NbSe_2$ ARPES data obtained along the G–K cut near the Γ point. The right panel shows the selected momentum distribution curves from the data in the left panel. Arrows mark the Fermi momenta of folded bands at the Γ point.

marked by arrows are very clear, confirming the presence of an electron-like band.

By comparing the folded (at Γ) and original (intense band between 0.4 and 0.6 Å^{-1}) bands, the folded band is observed to be much weaker. This indicates that the electron scattering due to the extra modulation induced by Fe atoms is not very strong. This is understandable considering the fact that the electrons that form the bands are located within $NbSe_2$ and the magnetic moments are in the Fe atoms, that is, they are geometrically separated. Likewise, we may see additional band folding due to AF ordering. This is more plausible because the temperature-dependent resistivity data in Fig. 3 indicate that coupling between an electron and an Fe magnetic moment can be fairly strong. However, folded bands due to the AF order were not observed in our data. This shows that the effect of the AF order is not as strong as that of the atomic order.

© 2013 The Japan Society of Applied Physics

4. Conclusions

We grew single crystals of Fe_xNbSe_2 $(x = 0, 0.25)$ and Cu_xNbSe_2 $(x = 0, 0.06)$ by the iodine vapor transport method. The crystallinity of the single crystals was confirmed by XRD analysis. The c-axis lattice constant determined from the XRD measurement increases upon intercalation, indicating that atoms are indeed inserted between $NbSe_2$ layers. ARPES experiments were performed to measure the electronic structures of the samples. We observed, judging from the amount of downshift in the band structure, that a significant number of electrons are doped to $NbSe_2$. In addition, we observed band folding due to Fe atom ordering for Fe_xNbSe_2. However, we did not observe the effect of the Fe magnetic moment AF order in spite of the fact that fairly strong electron-magnetic moment scattering is suggested from the resistivity data. This indicates that electron coupling to the AF order is not as strong as that to the Fe atom order.

Acknowledgements

This work was supported by NRF (Contract No. 20090080739), the A3 Foresight Program through the NRF of Korea funded by MEST and the Converging Research Center Program through the Ministry of Science, ICT and Future Planning, Korea (2013K000312).

1) A. H. Castro Neto, F. Guinea, N. M. R. Peres, K. S. Novoselov, and A. K. Geim: Rev. Mod. Phys. **81** (2009) 109.
2) A. K. Geim: Science **324** (2009) 1530.
3) A. K. Geim and K. S. Novoselov: Nat. Mater. **6** (2007) 183.
4) K. S. Novoselov, A. K. Geim, S. V. Morozov, D. Jiang, Y. Zhang, S. V. Dubonos, I. V. Grigorieva, and A. A. Firsov: Science **306** (2004) 666.
5) K. S. Novoselov, A. K. Geim, S. V. Morozov, D. Jiang, M. I. Katsnelson, I. V. Grigorieva, S. V. Dubonos, and A. A. Firsov: Nature **438** (2005) 197.
6) S. Stankovich, D. A. Dikin, G. H. B. Dommett, K. M. Kohlhaas, E. J. Zimney, E. A. Stach, R. D. Piner, S. T. Nguyen, and R. S. Ruoff: Nature **442** (2006) 282.
7) N. Mingo and D. A. Broido: Phys. Rev. Lett. **95** (2005) 096105.
8) S. Ghosh, W. Bao, D. L. Nika, S. Subrina, E. P. Pokatilov, C. N. Lau, and A. A. Balandin: Nat. Mater. **9** (2010) 555.
9) I. Meric, M. Y. Han, A. F. Young, B. Ozyilmaz, P. Kim, and K. L. Shepard: Nat. Nanotechnol. **3** (2008) 654.
10) T. Ohta, A. Bostwick, T. Seyller, K. Horn, and E. Rotenberg: Science **313** (2006) 951.
11) Y. Zhang, T.-T. Tang, C. Girit, Z. Hao, M. C. Martin, A. Zettl, M. F. Crommie, Y. R. Shen, and F. Wang: Nature **459** (2009) 820.
12) J. B. Oostinga, H. B. Heersche, X. Liu, A. F. Morpurgo, and L. M. K. Vandersypen: Nat. Mater. **7** (2008) 151.
13) E. V. Castro, K. S. Novoselov, S. V. Morozov, N. M. R. Peres, J. M. B. Lopes dos Santos, J. Nilsson, F. Guinea, A. K. Geim, and A. H. C. Neto: Phys. Rev. Lett. **99** (2007) 216802.
14) G. Giovannetti, P. A. Khomyakov, G. Brocks, P. J. Kelly, and J. van den Brink: Phys. Rev. B **76** (2007) 073103.
15) N. Kharche and S. K. Nayak: Nano Lett. **11** (2011) 5274.
16) F. Levy: *Intercalated Layered Materials* (D. Reidel Publishing, Dordrecht, 1979) Part 1, p. 251.
17) B. Radisavljevic, A. Radenovic, J. Brivio, V. Giacometti, and A. Kis: Nat. Nanotechnol. **6** (2011) 147.
18) J. M. E. Harper, T. H. Geballe, and F. J. Di Salvo: Phys. Lett. A **54** (1975) 27.
19) J. J. Hauser, M. Robbins, and F. J. DiSalvo: Phys. Rev. B **8** (1973) 1038.
20) R. C. Morris: Phys. Rev. Lett. **34** (1975) 1164.
21) W. Z. Hu, G. T. Wang, R. Hu, C. Petrovic, E. Morosan, R. J. Cava, Z. Fang, and N. L. Wang: Phys. Rev. B **78** (2008) 085120.
22) F. J. Di Salvo, J. A. Wilson, B. G. Bagley, and J. V. Waszczak: Phys. Rev. B **12** (1975) 2220.
23) E. Morosan, H. W. Zandbergen, B. S. Dennis, J. W. G. Bos, Y. Onose, T. Klimczuk, A. P. Ramirez, N. P. Ong, and R. J. Cava: Nat. Phys. **2** (2006) 544.
24) K. E. Wagner, E. Morosan, Y. S. Hor, J. Tao, Y. Zhu, T. Sanders, T. M. McQueen, H. W. Zandbergen, A. J. Williams, D. V. West, and R. J. Cava: Phys. Rev. B **78** (2008) 104520.
25) Z. Dai, Q. Xue, Y. Gong, C. G. Slough, and R. V. Coleman: Phys. Rev. B **48** (1993) 14543.
26) S. J. Hillenius and R. V. Coleman: Phys. Rev. B **20** (1979) 4569.
27) J. F. Garvin, Jr. and R. C. Morris: Phys. Rev. B **21** (1980) 2905.
28) C. S. Oglesby, E. Bucher, C. Kloc, and H. Hohl: J. Cryst. Growth **137** (1994) 289.
29) E. Morosan, H. W. Zandbergen, L. Li, M. Lee, J. G. Checkelsky, M. Heinrich, T. Siegrist, N. P. Ong, and R. J. Cava: Phys. Rev. B **75** (2007) 104401.
30) A. Meerschaut and C. Deudon: Mater. Res. Bull. **36** (2001) 1721.

© 2013 The Japan Society of Applied Physics